Journal of Alloys and Compounds 712 (2017) 250–255

Contents lists available at ScienceDirect

Journal of Alloys and Compounds

journal homepage: http://www.elsevier.com/locate/jalcom

Composition dependence of mechanically-induced structural rejuvenation in Zr-Cu-Al-Ni metallic glasses

Jian Qiang [a, b, *], Koichi Tsuchiya [a, b, **]

[a] University of Tsukuba, 1-1-1 Tennodai, Tsukuba, Ibaraki, 305-8577, Japan
[b] National Institute for Materials Science, 1-2-1 Sengen, Tsukuba, Ibaraki, 305-0047, Japan

ARTICLE INFO

Article history:
Received 10 January 2017
Received in revised form
8 April 2017
Accepted 11 April 2017
Available online 12 April 2017

Keywords:
Metallic glasses
Structural rejuvenation
Mechanical properties
Calorimetry
Fragility

ABSTRACT

With the aim of studying the effect of composition on structural rejuvenation, high-pressure torsion was performed on $Zr_{55}Cu_{30}Ni_5Al_{10}$ and $Zr_{65}Cu_{18}Ni_7Al_{10}$ metallic glasses. Nanoindentation measurements showed that structural rejuvenation in these two alloys was accompanied by a transition in deformation mode from localized deformation to a more homogenous deformation. The rejuvenated samples also exhibited strain-softening and improved plasticity. The increase in relaxation enthalpy of $Zr_{55}Cu_{30}Ni_5Al_{10}$ metallic glasses was larger than that of $Zr_{65}Cu_{18}Ni_7Al_{10}$, indicating different extents of structural rejuvenation. The influence of composition on the extent of structural rejuvenation was assessed for different systems of metallic glasses in the literature from the perspective of atomic clusters and liquid fragility. It was concluded that metallic glasses formed from more fragile liquids could be more susceptible to mechanically-induced rejuvenation.

1. Introduction

Metallic glasses (MGs) possess many outstanding properties such as great strength, a high elastic limit and good resistance to corrosion that stem from their disordered atomic configuration. An MG of a specific composition can exist in many structural states depending on its thermal history and/or mechanical treatments [1,2]. Upon annealing, an MG experiences structural relaxation into a lower energy state with a more ordered structure [3]. In regards to application, structural relaxation should be avoided as it leads to weakened mechanical properties [3,4]. Contrarily, tuning the atomic structure to a higher energy state with greater disorder (*i.e.* structural rejuvenation) is of great interest. Structural rejuvenation can be defined as the excitation of atomic configuration towards a higher energy level, and can be quantified by measuring the increase in relaxation enthalpy (ΔH_{rel}) [3,5]. Recently, structural rejuvenation has been studied extensively in the hope of improving plasticity and gaining a better understanding of the structure of MGs at an atomic level [2,4–16].

Structural rejuvenation can be induced by thermal processes. Saida et al. demonstrated rejuvenation in $Zr_{55}Al_{10}Ni_5Cu_{30}$ MG by heating to a temperature slightly above the glass transition temperature (T_g) followed by a rapid cooling [7] which can be attributed to the change in the fraction of short-range orders [4]. Thermally induced rejuvenation can also be achieved by cryogenic treatment. Ketov et al. reported an increase in ΔH_{rel} of ~340 J/mol after thermal cycling $La_{55}Ni_{20}Al_{25}$ MG ribbon between room and liquid nitrogen temperatures [5]. They ascribed this phenomenon to a non-uniform coefficient of thermal expansion, whereas Greer and Sun suggested that rejuvenation in this case was caused by an endothermic disordering process [3].

Structural rejuvenation can also be achieved by mechanical means. Louzguine-Luzgin et al. found an effect similar to structural rejuvenation at the center of a $Zr_{61}Cu_{27}Fe_2Al_{10}$ MG rod after cyclic loading within the elastic limit [2]. Plastic deformation can also lead to rejuvenation as was observed in samples subjected to elastostatic compression [11], cold-rolling [12], laser peening [15] and even nano-scale forces exerted by atomic force microscopy [16]. Compared to these methods, severe plastic deformation techniques can drastically increase the strain level, therefore achieving a much higher level of rejuvenation. For example, deformation of $Zr_{50}Cu_{40}Al_{10}$ MG by high-pressure torsion (HPT) can lead to an increase in ΔH_{rel} as large as 1500 J/mol [6]. Structural

* Corresponding author. Research Center for Strategic Materials, National Institute for Materials Science, Tsukuba, Ibaraki, 305-0047, Japan.
** Corresponding author. Research Center for Strategic Materials, National Institute for Materials Science, Tsukuba, Ibaraki, 305-0047, Japan.
E-mail addresses: QIANG.Jian@nims.go.jp (J. Qiang), TSUCHIYA.Koichi@nims.go.jp (K. Tsuchiya).

http://dx.doi.org/10.1016/j.jallcom.2017.04.096
0925-8388/

rejuvenation induced by plastic deformation can generally be attributed to the topological and chemical disordering introduced by the massive formation of shear transformed zones.

The level of structural rejuvenation not only depends on processing conditions such as the strain level [6,12] and the temperature [17] of plastic deformation, but is also related to the nature of the processed MG. Greer and Sun [3] have proposed that the dynamics of a composition with a higher liquid fragility are more heterogeneous, and thus could lead to an easier rejuvenation. However, insight on this issue is still lacking, because most studies on rejuvenation primarily focus on exploring new rejuvenation methods [2,5,15], or the microstructural or property changes in one particular composition [7,12,18,19]. In the present study, structural rejuvenation was induced in $Zr_{55}Cu_{30}Ni_5Al_{10}$ (Zr55) and $Zr_{65}Cu_{18}Ni_7Al_{10}$ (Zr65) MGs by HPT. The changes in thermal and mechanical properties resulting from structural rejuvenation were examined. With the aim of finding a correlation between the chemical composition and structural rejuvenation, the level of rejuvenation of Zr55 and Zr65 MGs was compared with other compositions reported in the literature, regardless of whether they were mechanically and/or thermally processed.

2. Experimental

Cylindrical MG samples with a diameter of 10 mm were fabricated by the tilt-casting method. The as-cast rods were sliced into disks and then subjected to HPT deformation. The HPT deformation was conducted under a compressive pressure of 5 GPa at room temperature with a rotation speed of 1 rpm for various numbers of rotation (N). Microstructure observations of the deformed samples were conducted on a JEOL JEM-2100 transmission electron microscope (TEM) with an accelerating voltage of 200 kV. Thermal analysis and sample annealing were performed using a Perkin-Elmer Diamond differential scanning calorimeter (DSC) at a heating rate of 40 K/min under a nitrogen atmosphere. The crystalline phases of annealed samples were identified using X-ray diffraction (XRD, Rigaku TTR III) with Cu-K_α radiation. Nanoindentation measurements were performed using a Hysitron Triboindenter TI950 with a Berkovich indenter under a load-control mode. The indentation measurements were conducted in the following sequence: loading to the maximum load of 5 mN in 20 s, holding at the maximum load (20 s) and finally unloading (20 s). The indentation measurements were carried out 4 mm away from the center of the disk. At least 15 indents were performed on each sample. The elastic modulus and hardness were calculated using the Oliver and Pharr method [20].

3. Results

Fig. 1 shows TEM bright-field images and the corresponding diffraction patterns (inset) of the Zr55 and Zr65 samples deformed by HPT ($N = 50$). The salt-and-pepper contrast in the bright field image and the broad halo in the diffraction pattern indicate that both the samples remained amorphous after HPT deformation, without any signs of crystallization.

Representative DSC curves for the Zr55 and Zr65 samples in the as-cast state and deformed to $N = 50$ are presented in Fig. 2. The ΔH_{rel} was calculated from the area encircled by the 1st and the 2nd heating curves of DSC analysis. The ΔH_{rel} in both the Zr55 and Zr65 alloys increased with N (Fig. 3), similar to $Zr_{50}Cu_{40}Al_{10}$ alloy in Ref. [6]. In the case of Zr55 (Fig. 2(a) and (b)), the ΔH_{rel} was 85 J/mol in the as-cast state, which increased to 761 J/mol after 50 rotations, indicating significant structural rejuvenation induced by HPT. Besides the increase in ΔH_{rel}, there was also a decrease in the onset temperature of structural relaxation (T_{onset}, marked by an arrow in Fig. 2). This suggests that the disordered structures induced by HPT are thermally unstable. Upon further heating above T_g, crystallization proceeded through a single-peak exothermic reaction. The T_g remained unchanged, but the onset crystallization temperature (T_x) decreased from 773 K to 769 K after HPT, indicating a weaker thermal stability of the supercooled liquid. Similarly, for Zr65 (Fig. 2(c) and (d)), there was an increase in the ΔH_{rel} from 64 J/mol to 492 J/mol after 50 rotations. A decrease in T_{onset} could also be observed. More importantly, a small exothermic peak appeared at the lower temperature side of the main peak, which not only deteriorated the thermal stability of the supercooled liquid, but also changed the crystallization mode.

In this context, we analyzed the crystallization products. The as-cast and HPT-deformed ($N = 50$) Zr55 samples were heated up to 798 K, about 50 K higher than T_x, in the DSC furnace. Fig. 4(a) shows the XRD profiles of the annealed samples. In the case of both the as-cast and HPT annealed samples, the crystallization products were Zr_2Ni, Zr_2Al, Zr_2Cu and some unknown phases. In the case of Zr65 (Fig. 4(b)), HPT caused significant changes in the crystallization behavior. For the HPT-deformed sample ($N = 50$), heating to 754 K (between the 1st and the 2nd onset crystallization temperature, T_{x1} and T_{x2}) led to the precipitation of Zr_2Cu, Zr_6NiAl_2 and some unknown phases. Further heating to 847 K (~50 K over T_{x2}) led to the precipitation of Zr_2Ni. The same precipitates could be identified in the as-cast Zr65 sample after annealing at 847 K (~50 K over T_{x2}). However, the intensity of the peaks corresponding to Zr_2Ni was stronger. The precipitation of Zr_2Ni was clearly suppressed after HPT.

The structural rejuvenation induced by HPT also resulted in changes in the mechanical properties. Fig. 5(a) shows typical load-depth curves of the as-cast and HPT-deformed Zr55 samples. The maximum indentation depth increased with increasing N, signifying strain-softening by structural rejuvenation. Moreover, the pop-in behavior associated with discrete shear band bursts [21] disappeared in the sample deformed by 50 rotations,

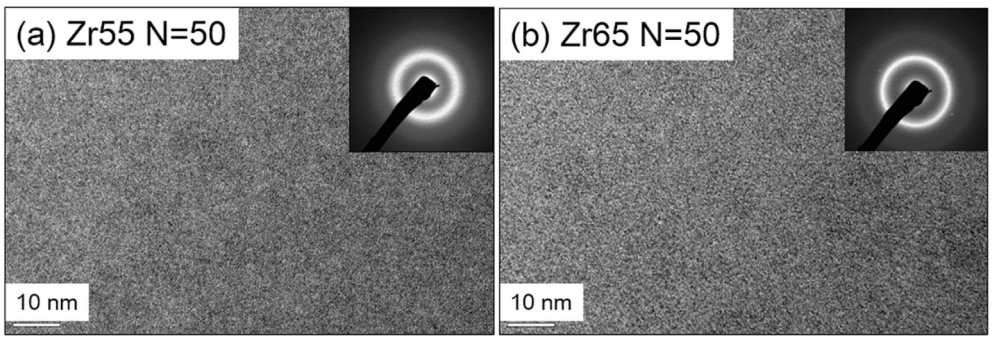

Fig. 1. Bright-field TEM images of Zr55 (a) and Zr65 (b) samples deformed by $N = 50$ rotations of HPT. The insets are corresponding selected area diffraction patterns.